Supporting Information

A Bioprobe Based on Aggregation Induced Emission (AIE) for Cell Membrane Tracking

Yuhao Li[a], Yongquan Wu[a], Jin Chang[b], Min Chen[a], Rui Liu[c]* and Fuyou Li[a]*

[a] Department of Chemistry, Fudan University, Shanghai 200433, P. R. China. [b] Discipline of Chemistry, Queensland University of Technology, Brisbane 4000, Australia. [c] College of Science, Nanjing University of Technology, Nanjing 210009, P. R. China.

Experimental section

Chemicals. All chemicals were purchased from Alfa-Aesar and Sinopharm Chemcial Reagent Co. Ltd. and were used without any further purification. Silica gel chromatography was carried out on silica gel (200-300 mesh). The intermediates 6-(7-bromo-9,9-dihexyl-9*H*-fluoren-2-yl)- 2-butyl-1*H* -benzo isoquinoline-1,3(2*H*)-dione (**1**) [1] and 4,4,5,5-tetramethyl-2-(naphthalen-2-yl)- 1,3,2-dioxaborolane (**2**) [2] were synthesized according to the literature methods.

Instrumentation. ^{1}H NMR and ^{13}C NMR spectra were obtained on a Varian Oxford-500 V NMR spectrometer, and proton chemical shifts were recorded in ppm down field from tetramethylsilane (TMS). High resolution mass spectra (HRMS) were measured on a voyager matrix assisted laser desorption/ionization-time of light mass spectrometer system. Elemental analysis was performed on a Vario EL III elemental analysis instrument and the results were within 0.5% of the calculated value. The Edinburgh LFS-920 fluorescence spectrometer with xenon lamp (450 W) as excitation

light source was utilized to obtain the steady-state emission spectra. The fluorescent quantum yields were determined by the comparative method,[3] in which a cyclohexane solution of 9,10-diphenylanthracene (DPA) (Φ_{em} = 0.97 ± 0.03, λ_{ex} = 355 nm) [4] was used as the reference. The emission lifetime were measured by Edinburgh ps-lifetime instrument with 355 ps laser as excited source. Dynamic light scattering (DLS) size was record on Zetasizer Nano ZS90. Artificial sun light was generated by short-arc xenon lamp (CHF-XM-500 W, Peikin Changtuo Science Co. Ltd.).

Calculations. To understand the nature of the ground state and the low-lying excited states of **FD-9**, quantum chemical calculations were performed for **FD-9**. All calculations were conducted at the DFT level of theory, in conjunction with the B3LYP functional [5,6] and the 6-31G* basis set [7-11], as implemented in the Gaussian 09 program package [12]. The geometry structure of **FD-9** in time-dependent DFT (TDDFT) calculation base on the gas phase optimized geometry.

Cell culture. The living HepG-2 cells were provided by the Institute of Biochemistry and Cell Biology, SIBS, CAS (China), which were grown in RPMI-1640 (Roswell Park Memorial Institute 1640) supplemented with 10% FBS (fetal bovine serum) and cultured at 37 ^{o}C under 5% CO_2.

Cytotoxicity assay. The cytotoxicity was measured using a standard methyl thiazolyl tetrazolium (3-(4,5-dimethyl-2-thiazolyl)-2,5-diphenyltetrazolium bromide, MTT, Sigma-Aldrich) assay in HepG-2 cell lines. Briefly, cells growing in log phase were seeded into 96-well cell-culture plate at 1×10^4 /well. The compound **FD-9** (100 μL/well) at concentrations of 10, 20, 30, 40, and 50 μM was added to the wells of the treatment group, and 100 μL/well DMSO diluted in RPMI-1640 at final

concentration of 0.2% to the negative control group, respectively. The cells were incubated for 24 h at 37 ^{o}C under 5% CO_2. The combined MTT/PBS solution was added to each well of the 96-well assay plate, and incubated for an additional 4 h. An enzyme-linked immunosorbent assay (ELISA) reader (infinite M200, Tecan, Austria) was used to measure the OD570 (Absorbance value) of each well referenced at 690 nm. The following formula was used to calculate the viability of cell growth:

Viability (%) = (mean of absorbance value of treatment group -mean absorbance value of control) × 100

Luminescence imaging.

For living cells imaging. Cells (5×10^8 /L) were plated on 14 mm glass coverslips and allowed to adhere for 24 h. The cells were washed with PBS and then incubated solely with 5 μM **FD-9** in DMSO/RPMI-1640 (1:49, v/v) for 30 min at 37 ^{o}C. Cells imaging were then carried out after washing cells with PBS (2 mL × 3 times).

For colocalization imaging of living cells. The HepG-2 cells were incubated with 15 μM **FD-9** in DMSO/RPMI-1640 (1:49, v/v) for 30 min at 37 ^{o}C, and then further incubated with **DiI** 5 μM for another 15 min before imaging.

For long-term tracking of living cells. Cells (1.8×10^5 /mL × 12 mL) incubated with 15 μM **FD-9** in DMSO/RPMI-1640 (1:49, v/v) for 30 min at 37 ^{o}C, then washed with RPMI-1640 and were grown in RPMI-1640 supplemented with 10% FBS and cultured at 37 ^{o}C under 5% CO_2. Cell imaging was then carried out after 1 d, 2 d, 3 d, and 4 d, respectively. After grown at 4 d, the cells number is 1.03×10^6 /mL × 12 mL. The incubated cells (4 day) and none-incubated (0 day) cells (1.24×10^7) were collected and distributed in 3 mL PBS (4.12×10^6/ mL), then intracellular

fluorescence was recorded (λ_{em} = 483 nm, λ_{ex} = 405 nm).

Luminescence imaging, including xy plane-scan, emission-scan, z plane-scan, and time-lapse imaging were performed with an Olympus FV1000 confocal fluorescence microscope and an 60× oil-immersion objective lens.[15] Cells incubated with **FD-9** were excited at 405 nm (2.85 μW) with a semiconductor laser, and the emission was collected at 480 ± 50 nm. And cells incubated with DiI were excited at 543 nm (2.25 μW) with a semiconductor laser, and the emission was collected at 600 ± 50 nm. Quantization by line plots was accomplished using the software package provided by Olympus instrument. Each of the experiments was performed at least 3 times.

Amphiphilicity of FD-9. The octanol/water partition coefficient, $P_{o/w}$ (or log $P_{o/w}$) represents the relative solubility of a given material in oil and water. The $P_{o/w}$ of FD-9 was measured on an HY-4 oscillator according to a classical method[13,14]. Equal amounts of n-octanol and H_2O were thoroughly mixed in the oscillator for 24 h. The mixture was then left to separate for a further 24 h so as to yield H_2O and octanol phase, each saturated with the other. Compound **FD-9** was carefully dissolved in H_2O (concentration denoted as C_o) and H_2O saturated with octanol to form a 4 μM solution. The latter was then mixed with an equal amount of octanol (saturated with water) and shaken again as described above. After separation, the final concentration of **FD-9** in water was denoted as C_w. Both C_o and C_w were measured by UV-Vis absorption spectroscopy at λ = 385 nm, and the $P_{o/w}$ for **FD-9** was calculated according to the equation: $P_{o/w} = (C_o - C_w) / C_w$.

Synthetic procedure of FD-9.

The synthetic routine of FD-9 shows in Scheme S1.

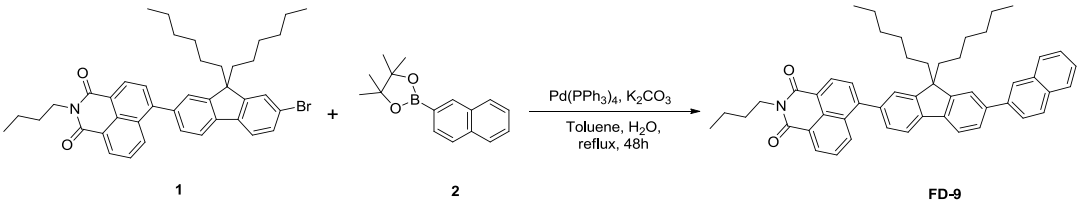

Scheme S1. Synthetic routine of **FD-9**.

Compound **1** (200 mg, 3.0 mmol), compound **2** (77 mg, 3.0 mmol) and $Pd(PPh_3)_4$ (21 mg, 0.018 mmol) were added to 30 mL of toluene. Then, 1 mL K_2CO_3 (2 M) aqueous solution was added. The mixture was heated to reflux under argon for 48 h. The mixture was then reduced in *vacuo*, extracted with CH_2Cl_2, washed by brine and the combined organic layer was dried over $MgSO_4$. After removal of the solvent, the crude product was purified by column chromatography (silica gel, 200-300 mesh) using hexane/ether (20:1, v/v) as the eluent, yellow-green product (yield 70%) was obtained. ^{1}H NMR (500 MHz, $CDCl_3$) δ 8.67 (dd, J_1 = 15.6 Hz, J_2 = 7.3 Hz, 2H), 8.34 (d, J = 8.5 Hz, 1H), 8.13 (s, 1H), 7.96 (t, J = 8.3 Hz, 2H), 7.90 (t, J = 8.0 Hz, 3H), 7.85 (d, J = 8.7 Hz, 1H), 7.80 (d, J = 7.5 Hz, 1H), 7.77 (d, J = 7.9 Hz, 1H), 7.73 (s, 1H), 7.70 (t, J = 7.9 Hz, 1H), 7.53 (dd, J_1 = 17.0 Hz, J_2 = 7.8 Hz, 4H), 4.28–4.19 (m, 2H), 2.16–2.02 (m, 4H), 1.82–1.71 (m, 2H), 1.54–1.43 (m, 2H), 1.17–1.07 (m, 12H), 1.01 (t, J = 7.4 Hz, 3H), 0.79 (m, 10H). ^{13}C NMR (126 MHz, $CDCl_3$) δ 164.62, 164.43, 152.07, 151.76, 147.71, 141.48, 140.86, 139.91, 139.07, 137.67, 133.98, 132.92, 132.88, 131.39, 131.09, 130.50, 129.14, 129.07, 128.71, 128.40, 128.11, 127.92, 126.94, 126.81, 126.63, 126.21, 126.00, 125.93, 124.81, 123.25, 122.11, 121.87, 120.65, 120.22, 55.72, 40.57, 40.55, 31.73, 30.50, 29.90, 24.17, 22.80, 20.67, 14.25, 14.12. HRMS $(M+H)^+$ calcd, m/z = 712.4076; found, m/z = 712.4099. Anal. calcd C 86.04, H 7.50, N 1.97, found C 86.14, H 7.55, N 2.00.

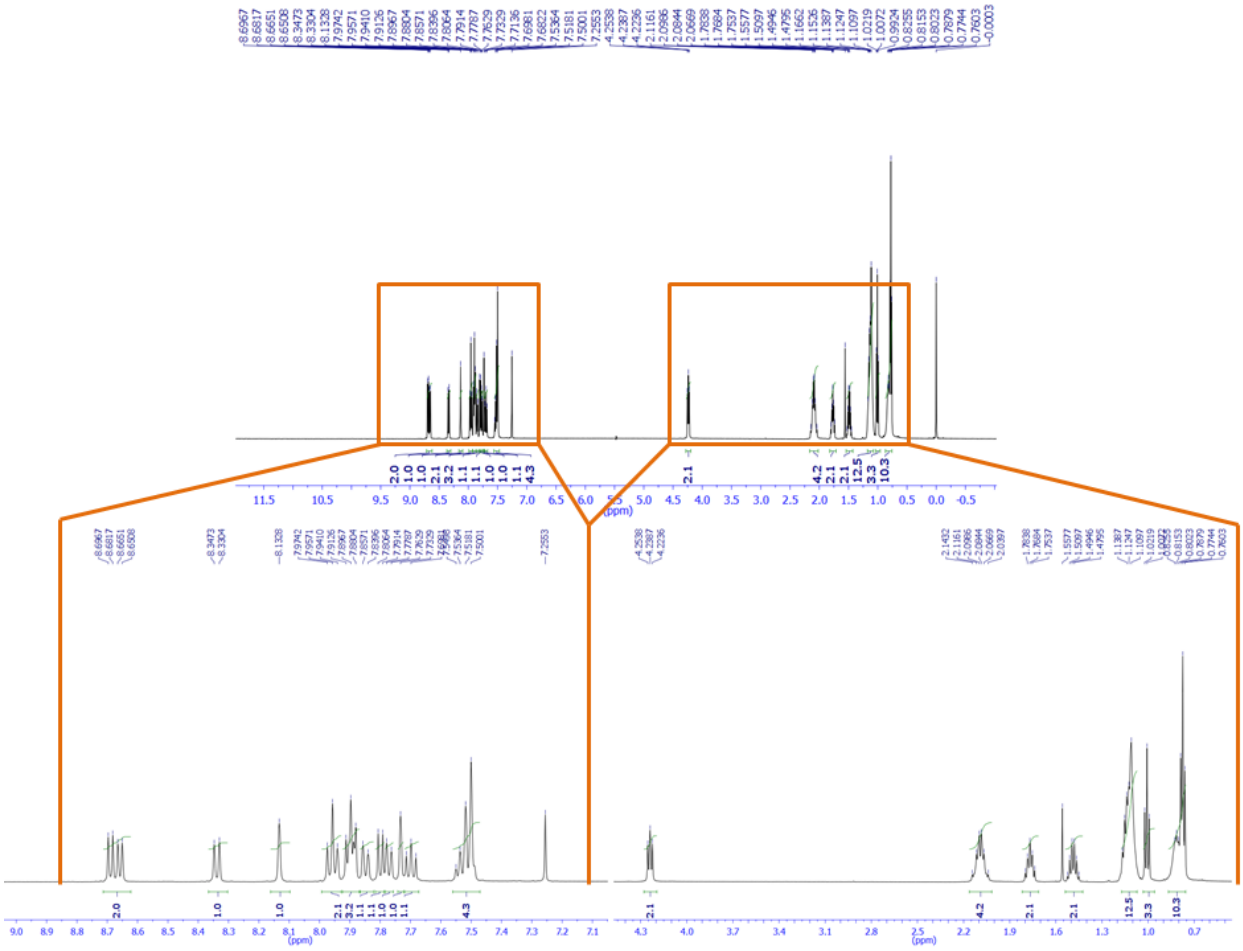

Figure S1. ^{1}H NMR spectrum of compound **FD-9**.

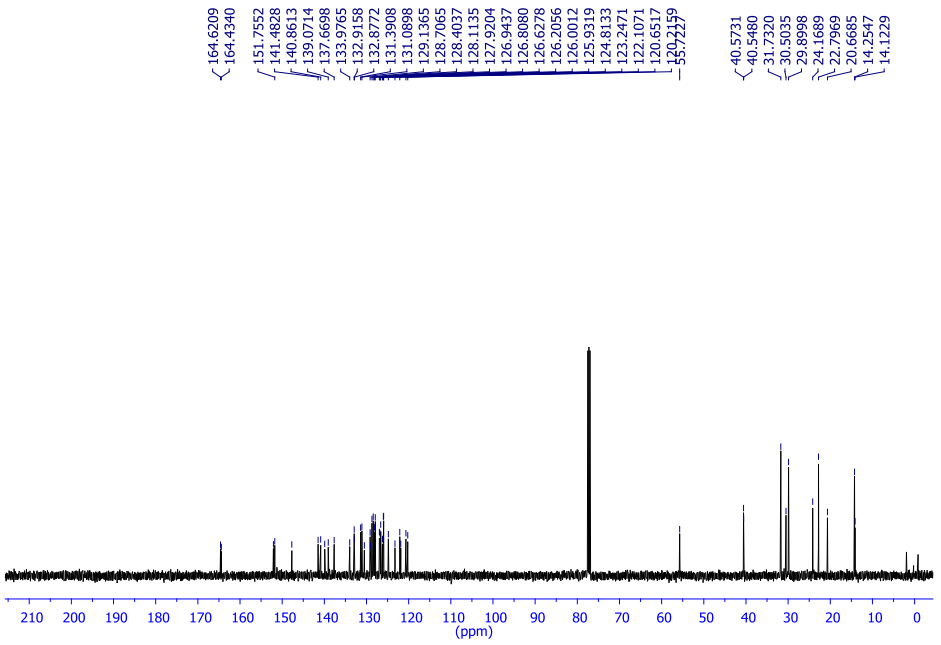

Figure S2. ^{13}C NMR spectrum of compound **FD-9**.

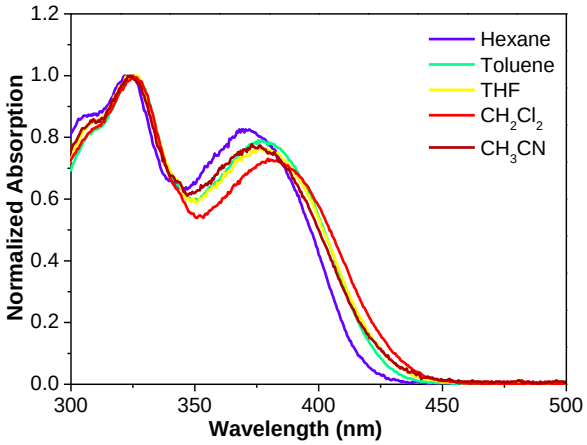

Figure S3. Normalized absorption spectra of **FD-9** in different solvents.

Table S1. Photophysical parameters of **FD-9** in different solvents.

solvent	λ_{em}/ nm	Φ_{em}	τ_{em}/ ns
Hexane	446	64.2%	11.04 (68.71%), 1.84 (31.29%)
Toluene	459	64.2%	10.50 (53.57%), 1.46 (46.43%)
THF	497	48.5%	11.45 (10.71%), 1.99 (89.29%)
CH_2Cl_2	513	48.0%	13.51 (5.66%), 2.58 (94.34%)
CH_3CN	540	20.4%	3.17

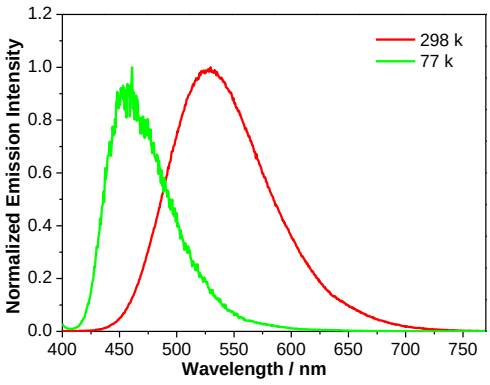

Figure S4. Normalized emission spectra of **FD-9** in BuCN at 298K and 77K, (λ_{ex} = 390 nm).

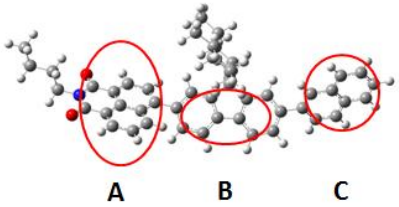

Compound	Twisted angle (AB)	Twisted angle (BC)	Dipole moment
FD-9	54.7^{o}	39.4^{o}	5.93

Figure S5. Optimized structure of **FD-9** in gas phase obtained at the B3LYP/6-31G* level of theory.

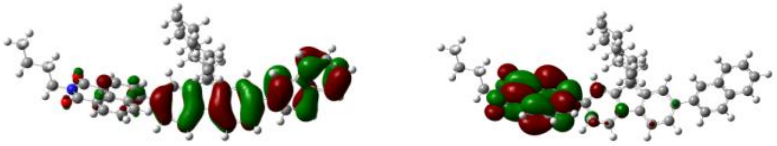

Figure S6. Contour plot of the highest occupied molecular orbital (HOMO) and lowest unoccupied molecular orbital (LUMO) for **FD-9** in gas phase obtained at the B3LYP/6-31G* level of theory.

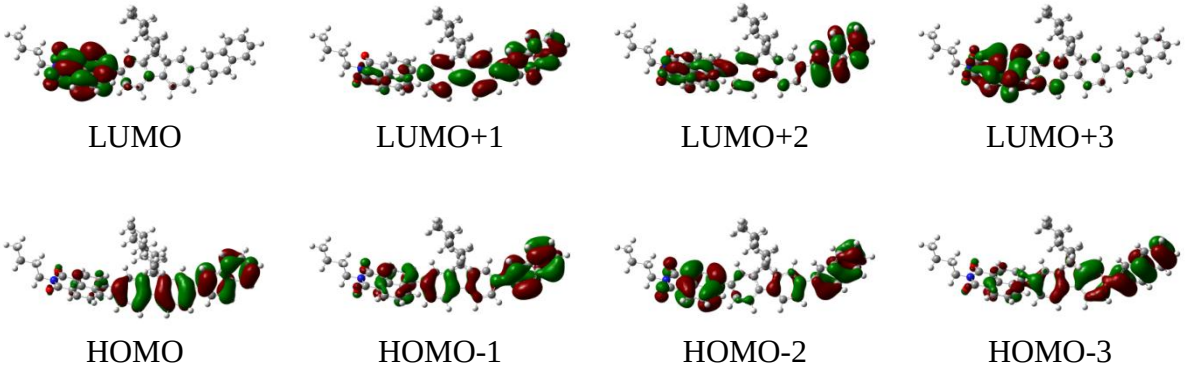

Figure S7. Frontier molecular orbitals of the compound **FD-9**. Calculated at the B3LYP/6-31G* level using Gaussian 09.

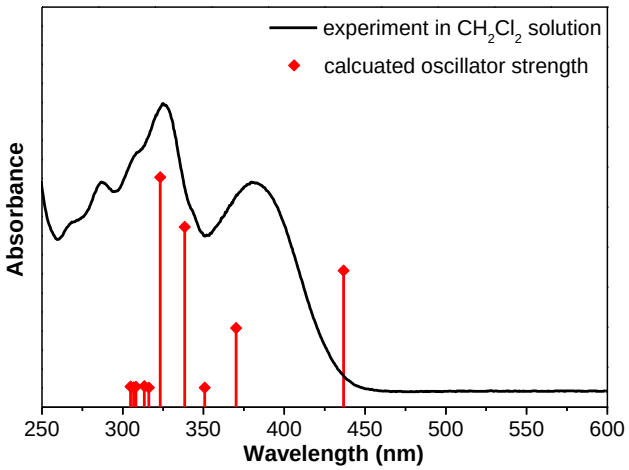

Figure S8. UV absorbance of **FD-9** in CH_2Cl_2 solution (experimentation, black), and calculated oscillator strength (calculation, red) in gas phase obtained at the B3LYP/6-31G* level of theory.

Table S2. Calcuated singlet-state parameters for **FD-9** by TDDFT, based on the ground state geometry optimized in gas phase.

	TDDFT/B3LYP/6-31G*			
Energy	f [a]	Composition [b]	CI [c]	Character [d]
2.8390 eV/ 436.71 nm	0.3087	H-1 → L	0.10909	ICT
		H → L	0.69516	ICT
3.3491 eV/ 370.21 nm	0.1579	H-1 → L	0.69208	ICT
		H → L	0.11435	ICT
3.5355 eV/ 350.68 nm	0.0012	H-5 → L	0.68518	ICT & $\pi\pi^*$
3.6638 eV/ 338.40 nm	0.4232	H-2 → L	0.66246	ICT & $\pi\pi^*$
		H → L+1	0.20968	ICT
3.8368 eV/ 323.15 nm	0.5535	H-2 → L	0.21102	ICT & $\pi\pi^*$
		H → L+1	0.66292	ICT
3.9217 eV/316.15 nm	0.0013	H-9 → L	0.37388	$\pi\pi^*$
		H-7 → L	0.41759	ICT & $\pi\pi^*$
		H-6 → L	0.28854	ICT & $\pi\pi^*$
		H-4 → L	0.22637	ICT
3.9563 eV/ 313.38 nm	0.0053	H-9 → L	0.21406	$\pi\pi^*$
		H-7 → L	0.26042	$\pi\pi^*$ & ICT
		H-6 → L	0.31337	ICT & $\pi\pi^*$
		H-4 → L	0.49582	ICT
		H-3 → L	-0.15482	ICT & $\pi\pi^*$
4.0233 eV/ 308.16 nm	0.0034	H-9 → L	0.45245	$\pi\pi^*$
		H-8 → L	0.30239	$\pi\pi^*$
		H-7 → L	0.31653	$\pi\pi^*$ & ICT
		H-6 → L	0.12261	ICT & $\pi\pi^*$
		H-4 → L	0.13496	ICT
4.0434 eV/ 306.63 nm	0.0019	H-3 → L	0.40179	ICT & $\pi\pi^*$
		H-2 → L+1	0.11521	ICT & $\pi\pi^*$
		H-1 → L+1	0.37204	$\pi\pi^*$
		H → L+2	0.32364	ICT & $\pi\pi^*$
		H → L+4	0.12733	ICT & $\pi\pi^*$
4.0668 eV/ 304.87 nm	0.0042	H-7 → L	0.12500	$\pi\pi^*$ & ICT
		H-3 → L	0.52542	ICT & $\pi\pi^*$
		H-2 → L+1	0.11113	ICT & $\pi\pi^*$
		H-1 → L+1	0.25647	$\pi\pi^*$
		H → L+2	0.28254	ICT & $\pi\pi^*$

[a] Oscillator strength. [b] main composition, and H stands for HOMO and L stands for LUMO. [c] The CI coefficients are in absolute values. [d] "ICT" means intra-molecular charge transfer; "$\pi\pi^*$" means $\pi\pi^*$ charge transfer.

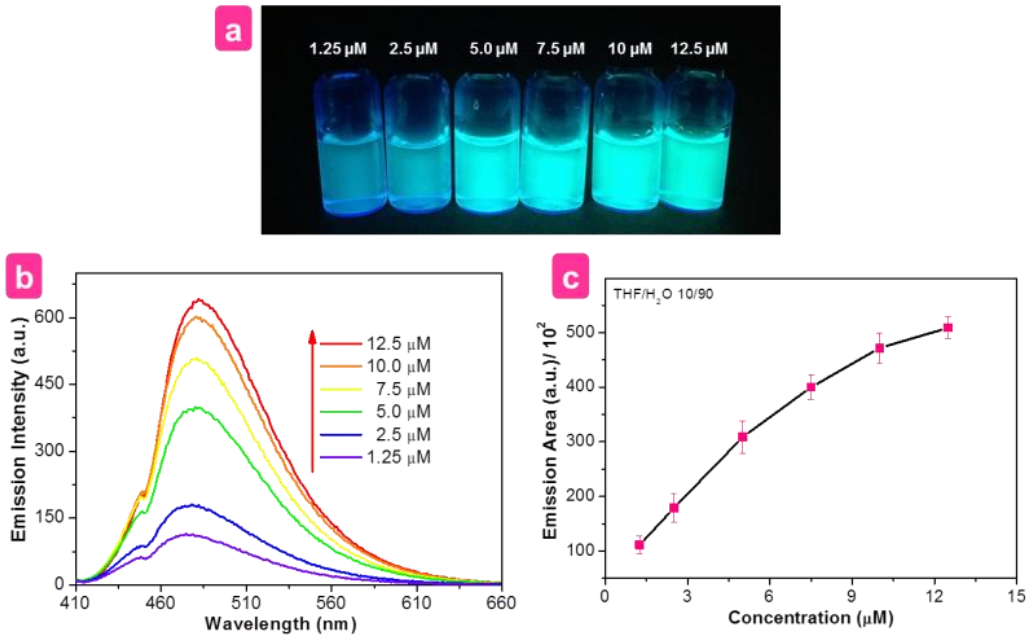

Figure S9. a) Digital photos of **FD-9** in different concentration (1.25 μM - 12.5 μM) in THF/H_2O mixture (1:9, v/v) under irradiation of UV lamp at 365 nm. b) Fluorescence spectrum of **FD-9** with different concentration (1.25 μM - 12.5 μM) in THF/H_2O mixture (1:9, v/v), λ_{ex} = 400 nm. c) Plot of fluorescent intensity of **FD-9** at 487 nm versus concentration of **FD-9** in THF/H_2O mixture (1:9, v/v), λ_{ex} = 400 nm.

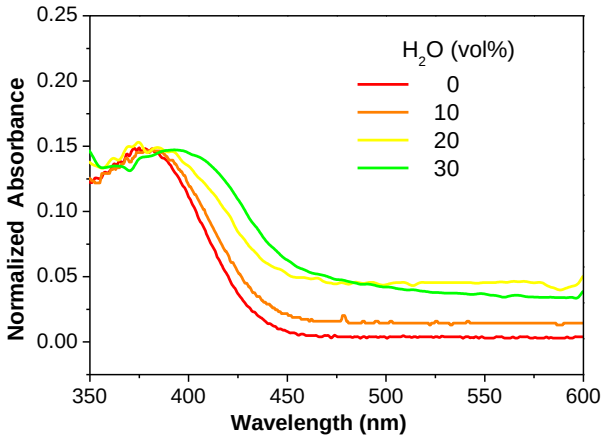

Figure S10. Normalized absorption spectra of **FD-9** (30 μM) in CH_3OH/H_2O (v/v) mixture with different H_2O fraction (vol%).

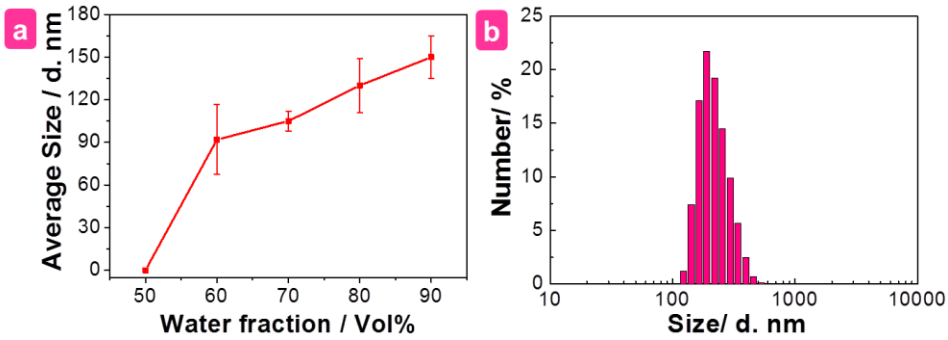

Figure S11. (a) Variation of the aggregate size of **FD-9** with the H_2O content of THF/H_2O (v/v) mixture. (b) Dynamic light scattering (DLS) of the **FD-9** nanoparticles formed in the THF/H_2O (1:9, v/v) mixture.

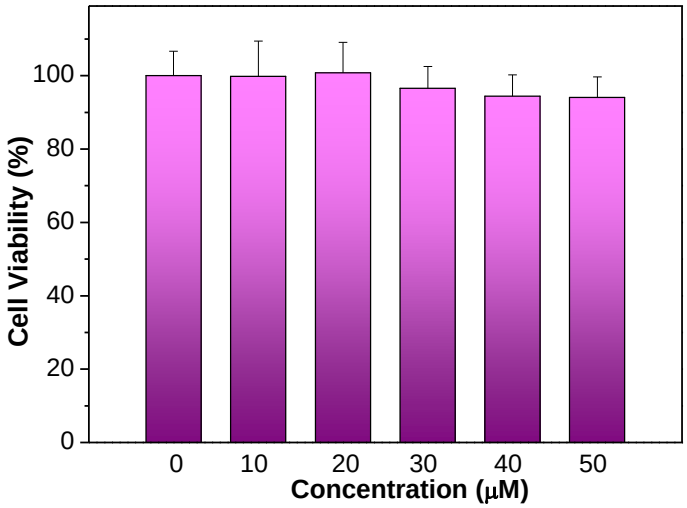

Figure S12. Cell viability values (%) estimated by MTT proliferation tests versus incubation concentrations of **FD-9**. HepG-2 cells were incubated with 0-50 μM **FD-9** at 37 ^{o}C for 24 h.

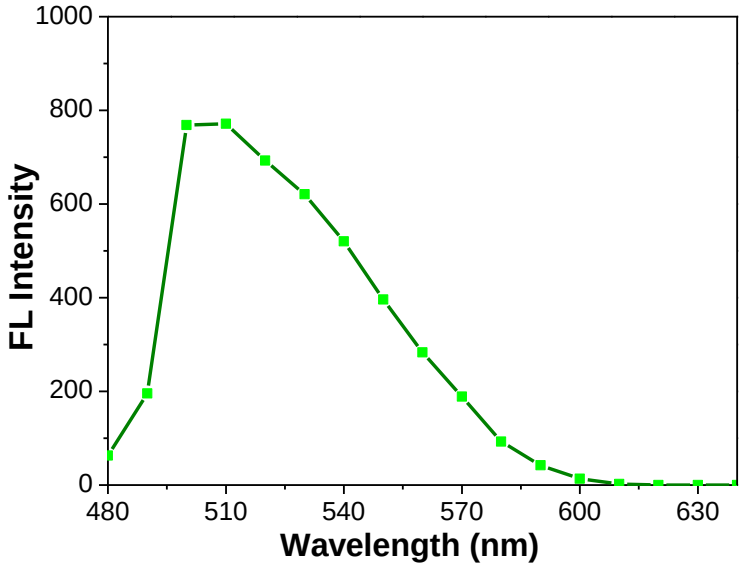

Figure S13. Emission spectrum of the **FD-9** incubated with HepG-2 cells, (λ_{ex} = 405 nm).

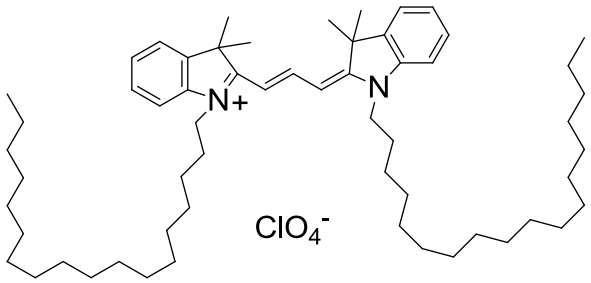

CAS: 41085-99-8

Name: 1,1'-dioctadecyl-3,3,3',3'-tetrameindo-carbocyan perchlora (**DiI**)

Figure S14. Chemical structure of **DiI**.

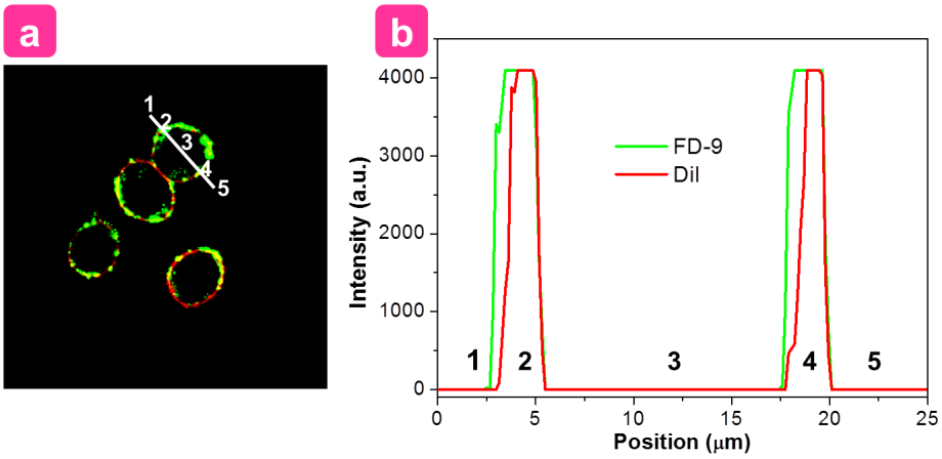

Figure S15. a) The confocal fluorescence imaging of living HepG-2 cells incubated with 5 μM **FD-9** (green, λ_{ex} = 405 nm, λ_{em} = 480 ± 50 nm) for 30 min and 5 μM DiI (red, λ_{ex} = 532 nm, λ_{em} = 600 ± 50 nm) for 15 min in DMSO/RPMI-1640 (1:49, v/v) at 37 ^{o}C. b) Luminescence intensity shows the confocal fluorescence imaging corresponding to Fig. S17(a) extracellular region (1 and 5), cell membrane (2 and 4), and cytoplasm and nuclear region (3).

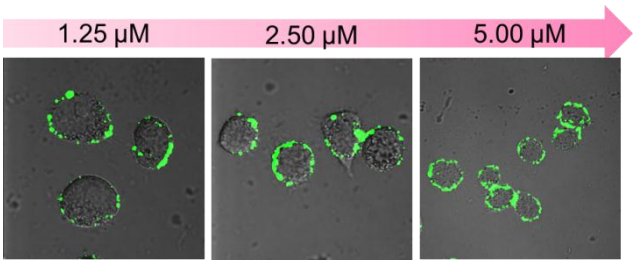

Fig. S16. The confocal fluorescence imaging of living HepG-2 cells incubated with **FD-9** (green, λ_{ex} = 405 nm, λ_{em} = 480 ± 50 nm) for 30 min in different concentration from 1.25 μM to 5 μM.

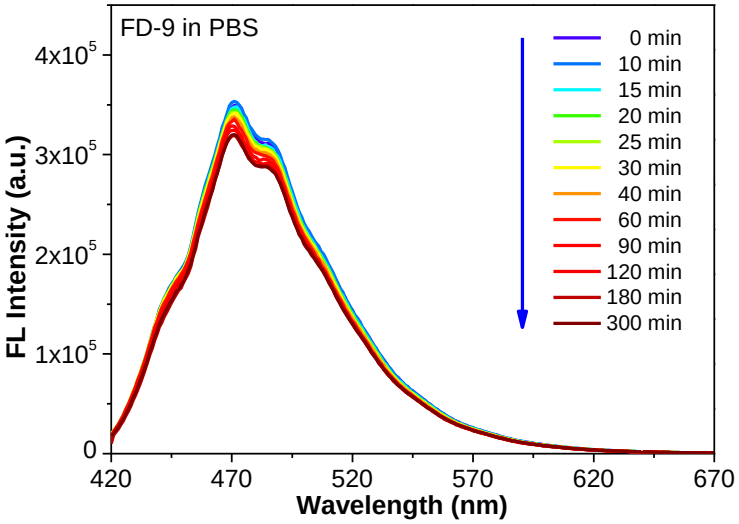

Figure S17. The emission changing of **FD-9** (5 μM) in DMSO/PBS (1:49, v/v) after irradiation of short-arc xenon lamp (CHF-XM-500 W) with different time.

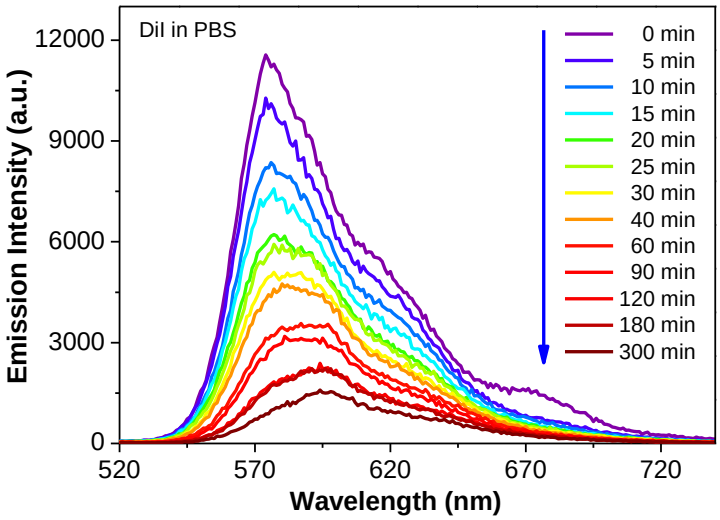

Figure S18. The emission changing of **DiI** (5 μM) in DMSO/PBS (1:49, v/v) after irradiation of short-arc xenon lamp (CHF-XM-500 W) with different time.

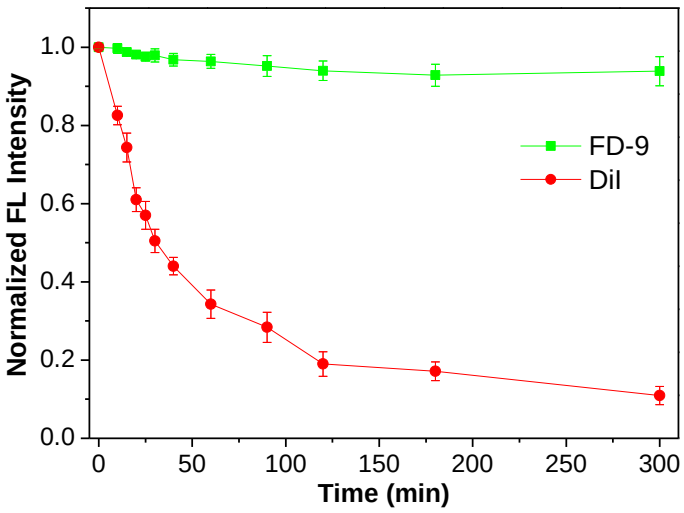

Figure S19. The intensity change in emission of **FD-9** at 470 nm and **DiI** at 580 nm after irradiation of short-arc xenon lamp (CHF-XM-500 W).

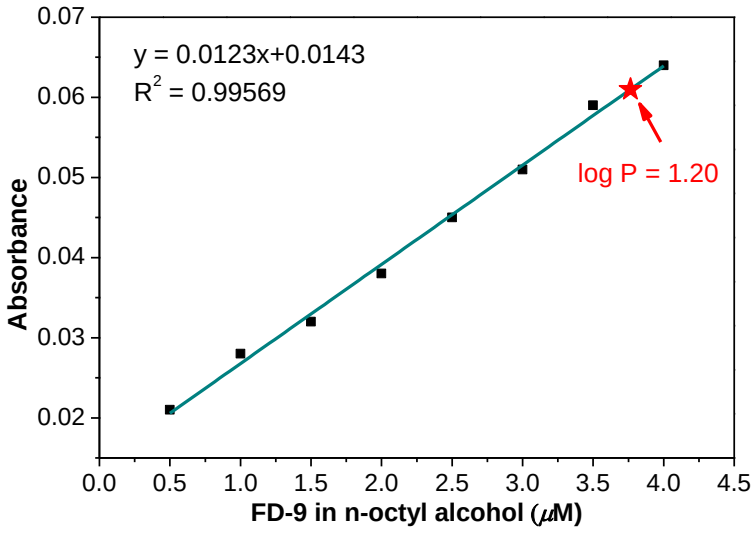

Figure S20. Log P of compound **FD-9**.

Reference:

[1] R. Liu, A. Azenkeng, Y. Li and W. Sun, *Dalton Trans.*, 2012, **41**, 12353.

[2] R. Liu, N. Dandu, Y. Li, S. Kilina and W. Sun, *Dalton Trans.*, 2013, **42**, 160.

[3] G. A. Crosby and J. N. Demas, *J. Phys. Chem.*, 1971, 991.

[4] K. Suzuki, A. Kobayashi, S. Kaneko, K. Takehira, T. Yoshihara, H. Ishida, Y. Shiina, S. Oishic

and S. Tobita, *Phys. Chem. Chem. Phys.*, 2009, **11**, 9850.

[5] D. B. Axel, *J. Chem. Phys.*, 1993, **98**, 5648.

[6] C. Lee, W. Yang and R. G. Parr, *Phys. Rev. B*, 1988, **37**, 785.

[7] T. Clark, J. Chandrasekhar, G. W. Spitznagel and P. V. R. Schleyer, *J. Comput. Chem.*, 1983, **4**, 294.

[8] M. M. Francl, W. J. Pietro, W. J. Hehre, J. S. Binkley, M. S. Gordon, D. J. DeFrees and J. A. Pople, *J. Chem. Phys.*, 1982, **77**, 3654.

[9] P. M. W. Gill, B. G. Johnson, J. A. Pople and M. J. Frisch, *Chem. Phys. Lett.*, 1992, **197**, 499.

[10] P. C. Hariharan, J. A. Pople, *Theor. Chim. Acta*, 1973, **28**, 213.

[11] R. Krishnan, J. S. Binkley, R. Seeger and J. A. Pople, *J. Chem. Phys.*, 1980, **72**, 650.

[12] M. J. Frisch, G. W. Trucks, H. B. Schlegel, G. E. Scuseria, M. A. Robb, J. R. Cheeseman, G. Scalmani, V. Barone, B. Mennucci, G. A. Petersson, H. Nakatsuji, M. Caricato, X. Li, H. P. Hratchian, A. F. Izmaylov, J. Bloino, G. Zheng, J. L. Sonnenberg, M. Hada, M. Ehara, K. Toyota, R. Fukuda, J. Hasegawa, M. Ishida, T. Nakajima, Y. Honda, O. Kitao, H. Nakai, T. Vreven, J. A. Montgomery Jr., J. E. Peralta, F. Ogliaro, M. Bearpark, J. J. Heyd, E. Brothers, K. N. Kudin, V. N. Staroverov, R. Kobayashi, J. Normand, K. Raghavachari, A. Rendell, J. C. Burant, S. S. Iyengar, J. Tomasi, M. Cossi, N. Rega, J. M. Millam, M. Klene, J. E. Knox, J. B. Cross, V. Bakken, C. Adamo, J. Jaramillo, R. Gomperts, R. E. Stratmann, O. Yazyev, A. J. Austin, R. Cammi, C. Pomelli, J. W. Ochterski, R. L. Martin, K. Morokuma, V. G. Zakrzewski, G. A. Voth, P. Salvador, J. J. Dannenberg, S. Dapprich, A. D. Daniels, Ö. Farkas, J. B. Foresman, J. V. Ortiz, J. Cioslowski and D. J. Fox, Revision A.1, Gaussian, Inc., Wallingford CT, 2009.

[13] D. J. Minick, J. H. Frenz, M. A. Patrick and D. A. Brent, *J. Med. Chem.*, 1988, **31**, 1923.

[14] J. Sansgter, Octanol-Water Partition Coefficients: Fundamentals and Physical Chemistry; Wiley: Chichester, 1997.

[15] M. Yu, F. Li, Z. Chen, H. Hu, C. Zhan, H. Yang and C. Huang, *Anal. Chem.*, 2009, **81**, 930.